Thermodynamics of Methane, Propane, and Carbon Dioxide Hydrates in Porous Glass

Duane H. Smith
National Energy Technology Laboratory, U.S. Department of Energy, Morgantown, WV 26507

and

Dept. of Physics, West Virginia University, Morgantown, WV 26506

Kal Seshadri
National Energy Technology Laboratory, Parsons Infrastructure and Technology Laboratory, Morgantown, WV 26505

Tsutoma Uchida
Institute for Energy Utilization, National Institute of Advanced Industrial Science and Technology (AIST), Sapporo 062-8517, Japan

Joseph W. Wilder
Dept. of Mathematics, West Virginia University, Morgantown, WV 26506

and

National Energy Technology Laboratory, U.s. Department of Energy, Morgantown, WV 26507

DOI 10.1002/aic.10141
Published online in Wiley InterScience (www.interscience.wiley.com).

Equilibrium pressure for the dissociation of methane, propane, or carbon dioxide hydrates confined in porous glass pores of nominal 15 nm radii were measured over a wide temperature range. A previously presented model is used to determine the pore radius involved at each temperature. Based on these results, pore volume distributions were reconstructed and compared with distributions obtained from nitrogen desorption isotherms. The analysis of the reported data indicate that for all three hydrates, nearly all of the sorbed water was converted to hydrate, but the amount of water taken up by the porous glass was less than that expected from nitrogen desorption studies. When propane was used to form hydrate, the pores not occupied by hydrate were involved in propane vapor–liquid equilibria. © 2004 American Institute of Chemical Engineers *AIChE J,* 50: 1589–1598, 2004
Keywords: desorption, vapor–liquid equilibria, dissociation, thermodynamics, pore volume distribution

Introduction

Gas hydrates belong to a class of compounds called clathrates, and are composed of water and low molecular weight compounds such as C1–C4 alkanes, carbon dioxide, hydrogen sulfide, or binary and higher mixtures of these gases. Water molecules, by the use of hydrogen bonds, form a framework containing large and small cavities. These cavities are occupied by gas molecules that stabilize the structure as a result of van der Waals forces. The structure of the gas hydrate depends on the guest molecule. Pure methane, for example, forms the sI structure, whereas a mixture of propane and methane, depend-

Correspondence concerning this article should be addressed to D. H. Smith.

ing on the relative composition of the two components, stabilizes the sII structure. The temperature and pressure at which the hydrate forms depends on the activity of water (van der Waals and Platteeuw, 1959).

Naturally occurring gas is often found in pores of natural sediments. When a gas–liquid interface occurs in a pore, the curvature of the interface causes the pressures on the two sides of the interface to differ by an amount called the *capillary pressure*; and this pressure difference changes many physical and chemical equilibria by significant amounts. For example, it is well known (Clennell et al., 1999; Henry et al., 1999) that the freezing point of pure water is depressed when confined in small pores; this reduction in the freezing point is accompanied by a reduction in the activity of the water. Similarly, the curvature of any interface between the different phases contained in the pores of a porous medium may shift the equilibria for formation and decomposition of gas hydrates in porous media by significant amounts. As originally suggested by Henry et al. (1999), and supported by subsequent experimental evidence, the interface relevant to interpreting hydrate equilibrium pressure shifts in porous media appears not to be *the gas–liquid interface*, but the interface between the hydrate and the aqueous phase (that is, liquid or solid water) present in the pores of the medium. The new experimental data presented below offer additional evidence for the belief that the hydrate–water interface is the one most relevant to the thermodynamics of hydrates in pores.

A laboratory study of the thermodynamics of hydrates in porous media was initiated by Handa and Stupin (1992). They investigated the properties of methane and propane hydrates in silica gel that had a broad pore-size distribution, with 7.0 nm as the nominal pore radius. For hydrate equilibria in porous media, each size of pore confers an additional degree of freedom, which can cause considerable difficulties in the interpretation of experimental data. Handa and Stupin recognized the existence of these complications and limited the interpretation of their data accordingly.

More recently, Uchida and coworkers (1999, 2002) published the results of their work on the properties of methane and other hydrates in porous glass of nominal pore radii of 5, 15, 25 nm, and other pore sizes. To alleviate the interpretational problems caused by the presence of a pore-size distribution, they devised a method to obtain the equilibrium for the mode size of pore in the sample. This allowed them to treat the relatively narrow distribution as "monodisperse." To determine the effect of pore size on the equilibrium, they used various glasses of different pore-size distributions and modes. The work of Handa and Stupin on hydrates in silica gel was expanded by Smith and coworkers (2002a,b), who investigated the equilibrium pressures, temperatures, and heats of formation of hydrates of methane, ethane, propane, or carbon dioxide in silica gels having broad pore-size distributions and nominal pore radii of 7.5, 5.0, 3.0, or 2.0 nm (about 16 combinations of different hydrates and pore-size distributions in all). They showed that the occurrence of multiple pore sizes could be used to calculate the thermodynamic surface of equilibrium pressure as a function of temperature and pore size, thus using all of the measured equilibrium pressure–temperature data. These researchers also recognized that, although this equilibrium surface did not depend on the extensive properties of an experiment, the path taken across it in each experiment did. Thus, for measurements to be fully interpretable, not only equilibrium pressures and temperatures, but also extensive properties such as head space volume and amount of hydrate initially formed, must be measured and reported (Wilder et al., 2001). However, although the combination of the experimental method of Handa and Stupin and the interpretational method of Smith et al. has been extensively applied to hydrates in silica gels, it had not been tested with experimental data on hydrates in other media, such as porous glass. Because of the role of extensive parameters in this approach, new experiments that included measurement of these parameters were needed.

This article reports equilibrium pressure–temperature data for the dissociation of methane-, propane-, or carbon dioxide–hydrate in porous glass having a nominal pore radius of 15 nm; for comparison with the previous work of Uchida et al., this porous glass was identical to that used in their previous work. The nominal pore size (15 nm) of the porous glass used in the present work is significantly larger than that of the silica gel (nominal 2, 3, 5, or 7.5 nm radii) previously reported in the literature (see Figure 1a). In addition to having a larger nominal pore radius, the porous glass also has a narrower (but finite) distribution of pore sizes, as can be seen in Figure 1a. Also reported here are the results of calculations of pore-size distributions from the observed phase equilibrium data.

Experimental Procedures

The preparation of the hydrates and the subsequent determination of the equilibrium pressure–temperature profiles for their dissociation were performed in a manner similar to that used previously by Seshadri and coworkers (2001) for silica gels with nominal 3.0-, 5.0-, or 7.5-nm pores. At each step of the experiment, the temperature in the cell was increased by a predetermined amount, and the gas pressure in the cell was measured after sufficient time has passed to allow the new equilibrium to be completely established.

Hydrates were formed in one of the same porous glasses (nominal pore radius of 15 nm) as previously used by Uchida and coworkers (2002) in some of their studies. The porous glass, as received, was saturated with water using the same procedure as described elsewhere (Seshadri et al., 2001) for silica gel: specifically, the glass was placed in a desiccator containing degassed, distilled water for a period of 4 to 6 days to prepare glass with sorbed water.

For comparison with size distributions calculated from the hydrate data, the pore-size distribution and pore volume of the porous glass were obtained from nitrogen desorption isotherms generated using Quantachrome Corp. Autosorb-1 equipment. The data reduction unit in this instrument calculates the mean pore radius and specific pore volume using the method proposed by Barrett, Jayner, and Halenda, sometimes referred to as the BJH method (Barrett et al., 1951). Because the output of the data reduction system did not include the pore-size distribution in a suitable graphical format, we computed the distribution from the desorption data using the BJH method as explained by Lowell and Shields (1991). The cumulative pore volume given by this method was slightly larger than the value generated by the instrument. The results given by the data reduction system in the instrument are the ones reported below.

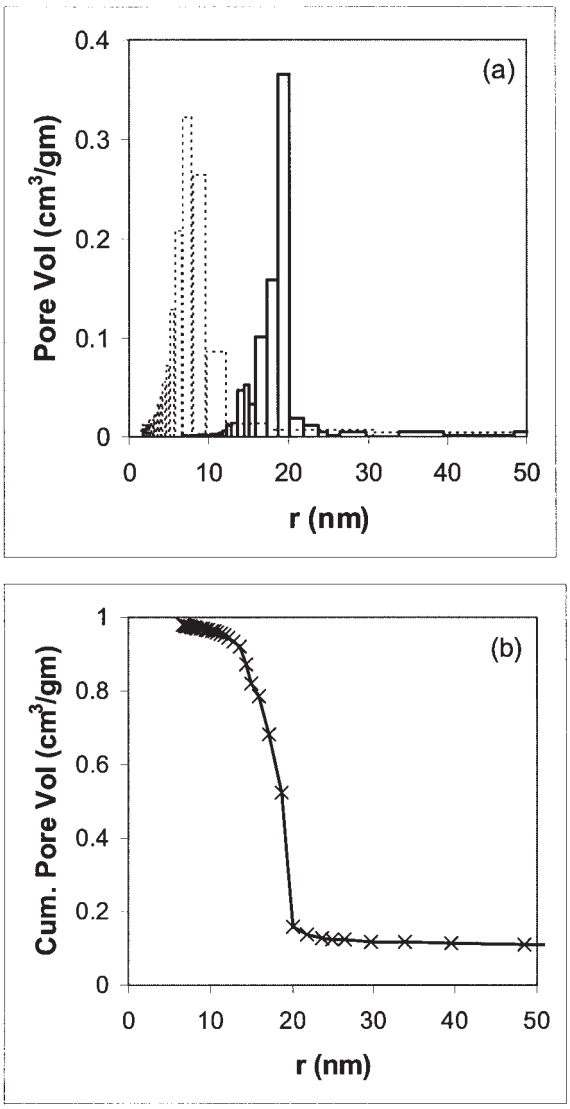

Figure 1. (a) Pore volume distributions for the nominal 15 nm pore radius porous glass used in this work (solid trace) as well as for the nominal 7.5 nm silica gel used in previous work (dotted trace); (b) cumulative pore volume for data of (a for the porous glass.

Note that the widths of the columns are not all the same because the lower and upper value of each range of radii, as well as the total pore volume within each range, are experimental points.

Results and Discussion

Measured hydrate equilibrium pressures are a function not just of the temperature, but also of the pore radius (Smith et al. 2002a; Wilder and Smith, 2002), unless the ranges of experimental radii and temperatures are very narrow. Therefore, the interpretation of the pressure and temperature data also requires that certain extensive parameters of the experiment be known (Wilder et al. 2001). These are listed in Table 1. Among the quantities of interest are the pore-size distribution of the glass, its total pore volume, the fraction of the total pore volume filled with water, and the fraction of the water converted to hydrate. In this investigation, nitrogen desorption yielded the specific pore volume 0.979 cm^3/g. This total pore volume includes 0.104 cm^3/g from pores of radius $\geq$ 114 nm. This is a significant fraction of the difference between the pore volume reported by Uchida and coworkers (1999) (0.796 cm^3/g) and that calculated from the nitrogen desorption isotherm. The pore volume as measured (gravimetrically) by the uptake of water was considerably less (0.624 cm^3/g) than that obtained from nitrogen desorption. Comparison of these pore volumes implies that only 64.25% of the total pore volume was filled with water. Using the amount of water in the glass (based on the water uptake), and assuming that the equilibrium composition of each of our hydrates was the same as for the bulk hydrate, we calculated the percentage conversion of water to hydrate; these values were 97.3, 95.0, and 83.4% for the methane, propane, and carbon dioxide hydrate, respectively. The fraction of the pore volume filled with water, but not the fraction of water converted to hydrate, was significantly less than the corresponding values found for silica gels.

There are two possible reasons for this difference between porous glass and silica gel. The first possible reason is (perhaps because of the surface groups on the glass) the complete filling of the pore space was hindered (relative to the silica gel) by its chemical properties (for a discussion of the properties of this glass, see Elmer, 1992). A second reason is that the pore-size distributions previously reported for the silica gels indicate that nearly all of the pore volumes were made up of pores with significantly smaller radii than those found in the porous glass. As a result, one would expect even the larger pores of the silica gel to be more readily filled than the majority of the pores in the porous glass because of the larger capillary forces resulting from the presence of smaller-radii pores. The pore-size distribution of the porous glass, as measured by nitrogen desorption, is plotted in Figure 1. Perhaps of more direct interest are the size distributions for the pores in which the various hydrates were formed. These are compared to each other and to the nitrogen-desorption pore-size distribution later in this work in Figure 6.

Tables 2–4 detail the observed equilibrium pressures at the indicated temperatures for hydrate formed from methane, propane, or carbon dioxide, respectively, in the nominal 15-nm radius porous glass. Although our experimental procedures were different, and although equilibrium pressure–temperature measurements will depend to some extent on the head space volumes and other extensive parameters of Table 1 (Wilder et al., 2001), the data in the present investigation and those previously reported by Uchida et al. (2002) appeared to be in substantial agreement.

Also shown in Tables 2–4 are the fugacities and the molar

Table 1. Sample Specifications

Property	Hydrate Sample		
	Methane	Propane	Carbon Dioxide
Net weight of porous glass saturated with water, g	5.5417	5.4223	7.0206
Water uptake of porous glass, g/g of glass	0.6239	0.6239	0.6239
Head space,* cm^3	21.23	21.43	17.97

* Includes the volume of the connecting tubes and values.

Table 2. Experimentally Measured Equilibrium Pressures (P) at the Indicated Temperatures (T) for Methane Hydrate in Nominal 15 nm Radius Porous Glass, and Molar Volumes (V_m) and Fugacities Calculated with the SRK Equation of State

T (K)	P (MPa)	$V_m \times 10^4$ (m^3/mol)	Fugacity (MPa)
266.15	2.20	9.48	2.08
267.15	2.23	9.37	2.11
268.15	2.28	9.21	2.15
269.15	2.38	8.83	2.25
270.15	2.51	8.38	2.36
271.15	2.70	7.80	2.53
272.15	2.91	7.24	2.71
273.15	3.10	6.79	2.88
274.15	3.32	6.35	3.07
275.15	3.59	5.86	3.30
276.15	3.79	5.55	3.47
277.15	3.81	5.54	3.50
279.15	3.85	5.54	3.54
281.15	3.88	5.54	3.57

volumes of the guest species in the vapor phase (V_m) at each of the experimental temperatures; both of these parameters were calculated using the Soave–Redlich–Kwong (Soave, 1972) equation of state. From the molar volume of the gas and the head space volume of the cell (the volume of the cell and the connecting tubes that is external to the sample and the glass beads), the number of moles of free gas in the cell at each temperature was calculated. Because the number of moles of gas in the head space at the final temperature (when the hydrate has all dissociated) represents the total amount of gas in the system, the difference between this final value (at the highest temperature) and the amount of gas in the vapor at any earlier temperature represents the moles of the gas that were sequestered in hydrate at the lower (earlier) temperature (total moles = moles in hydrate + moles in the head space).

Figures 2–4 show plots of the observed equilibrium pressures from the porous glass samples for methane, propane, or carbon dioxide hydrate, respectively, as well as data from

Table 3. Experimentally Measured Equilibrium Pressures (P) at the Indicated Temperatures (T) for Propane Hydrate in Nominal 15 nm Radius Porous Glass, and Molar Volumes (V_m) and Fugacities Calculated with the SRK Equation of State

T (K)	P (MPa)	$V_m \times 10^4$ (m^3/mol)	Fugacity (MPa)
269.15	0.204	10.53	0.196
270.15	0.231	9.29	0.221
271.15	0.245	8.77	0.234
272.15	0.272	7.88	0.258
273.15	0.313	6.82	0.295
274.15	0.369	5.74	0.344
275.15	0.431	4.87	0.398
276.15	0.497	4.18	0.453
277.15	0.539	3.83	0.488
278.15	0.559	3.70	0.505
279.15	0.587	3.51	0.528
280.15	0.607	3.40	0.544
281.15	0.627	3.29	0.561
282.15	0.648	3.18	0.578
283.15	0.661	3.13	0.589
285.15	0.689	3.01	0.612

Table 4. Experimentally Measured Equilibrium Pressures (P) at the Indicated Temperatures (T) for Carbon Dioxide Hydrate in Nominal 15 nm Radius Porous Glass, and Molar Volumes (V_m) and Fugacities Calculated with the SRK Equation of State

T (K)	P (MPa)	$V_m - 10^3$ (m^3/mol)	Fugacity (MPa)
263.15	0.70	2.97	0.67
265.15	0.77	2.71	0.73
266.15	0.82	2.54	0.78
267.15	0.86	2.43	0.81
268.15	0.92	2.27	0.86
269.15	1.00	2.09	0.94
270.15	1.08	1.93	1.01
271.15	1.18	1.76	1.09
272.15	1.28	1.62	1.18
273.15	1.39	1.48	1.27
274.15	1.51	1.36	1.37
275.15	1.66	1.23	1.49
276.15	1.68	1.22	1.51

Sloan (1997) for each of the corresponding bulk hydrates. As expected, for each temperature the equilibrium pressure is higher for the hydrate in the porous medium than it is for the bulk hydrate. For hydrates of methane and carbon dioxide apparent exceptions to this difference occur at higher temperatures because all of the hydrate is decomposed. The behavior of propane hydrate is discussed below. Also shown in these figures are equilibrium pressure data from the literature (Seshadri et al., 2001; Smith et al, 2002a,b) for hydrate equilibria in nominal 7.5-nm radius silica gel. We note that in all cases, the porous glass results lie between those for the silica gel and the bulk, as expected on the basis of a comparison of the nominal pore sizes.

We have three goals with respect to analyzing the data presented in Figures 2–4: (1) to determine the distribution of hydrate in the pores of the porous glass used in the experi-

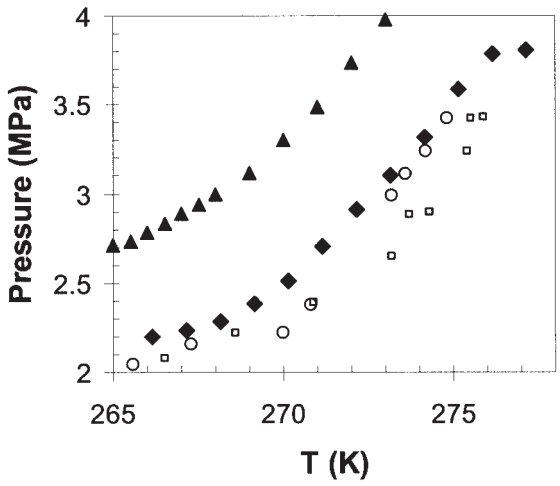

Figure 2. Measured equilibrium pressures (filled diamonds) for methane hydrate in porous glass with a nominal pore radius of 15 nm.

Also shown are data from the literature (open circles, Uchida et al. (1999)) using the same porous glass, data for 7.5 nm silica gel (filled triangles), and equilibrium pressures for bulk hydrate from Sloan (1997) (open squares).

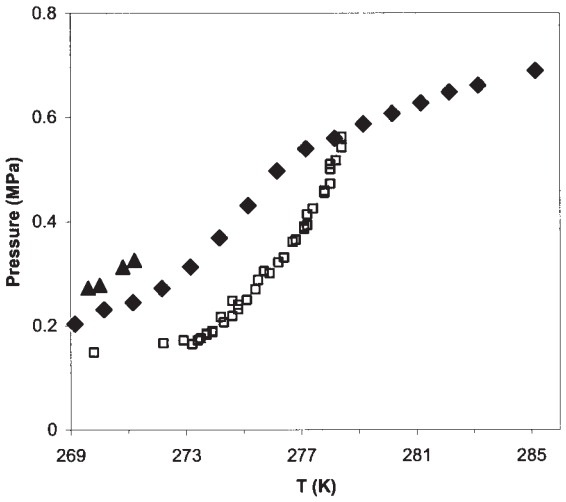

Figure 3. Measured equilibrium pressures (filled diamonds) for propane hydrate in porous glass with a nominal pore radius of 15 nm, and for 7.5 nm silica gel (filled triangles) from the literature.

Also shown are data for bulk hydrate from Sloan (1997) (open squares).

ments; (2) to compare the range of pore radii present in this porous glass and sampled in our experiments to those for other data reported in the literature for methane hydrate; and (3) to propose an explanation for the seemingly anomalous behavior of the propane hydrate data at temperatures above 278.15 K in Figure 3.

Hydrate distribution in the porous glass

Determination of the distribution of the hydrate in the porous glass requires an interpretive model for hydrate decomposition in porous media. The details of the model that will be used in this work are discussed in the Appendix. The model discussed therein can be used to determine the size of the hydrate containing pores that result in the observed equilibrium pressure at each experimental temperature (each experiment represents equilibrium not only for a unique P and T, but also for a unique pore radius). This information, along with the moles of hydrate dissociated between two consecutive temperatures can be used to construct the cumulative pore volume of the porous glass, as discussed below.

During temperature increase experiments, such as those performed here, the equilibrium pressure is measured at a series of increasing temperatures. The change in the number of moles of gas in the system in going from temperature T_i to T_{i+1} is given by

$$\Delta n_{i,i+1} = V_{sys}\left(\frac{1}{v_{i+1}} - \frac{1}{v_i}\right) \tag{1}$$

where V_{sys} is the volume of the free space in the cell (that is, the total volume of the cell minus that occupied by the porous glass and the hydrate it contains) and v_i is the molar volume of the gas at temperature T_i. The number of gas molecules contained in a unit cell of hydrate is n_{cell} and the volume of each unit cell is V_{cell}. When the pressure increases from P_i to P_{i+1}, the total volume (per gram of porous glass) of the pores from which the hydrate decomposed is

$$\Delta V_{i,j+1} = \frac{V_{cell}N_A}{n_{cell}w_{glass}}\Delta n_{i,j+1} = \frac{V_{cell}V_{sys}N_A}{n_{cell}w_{glass}}\left(\frac{1}{v_{i+1}} - \frac{1}{v_i}\right) \tag{2}$$

where w_{glass} is the weight of porous glass used in the experiment, and N_A is Avogadro's number. Given that V_{cell} is known and n_{cell} can be estimated based on the fractional occupancy of the cages (see Eq. A2), Eq. 2 gives an estimate of the volume of water involved in the formation of hydrate. In addition to the above calculation, Eq. A6 in the Appendix can be used to determine the radii r_i and r_{i+1} of the pores involved in the equilibria at the temperatures T_i and T_{i+1}, respectively. The combination of these radii with the volumes calculated with Eq. 2 allows for the estimation of the volume of hydrate contained in pores with radii in the range $r_i \le r \le r_{i+1}$. These volumes can then be used to construct Figure 5, which shows the pore-space volumes for pores having a radius of r or larger as a function of r, as calculated from the experimental methane, propane, or carbon dioxide hydrate equilibrium pressures reported in Tables 2–4 (for additional details concerning these calculations, see Smith et al. 2002a and Wilder et al. 2001). Also shown is the cumulative pore volume (Figure 1) from the nitrogen desorption measurements.

As can be seen in Figure 5, the distribution of hydrate in the porous glass was not uniform. If one compares the total (smallest pore radius) cumulative pore volumes shown in Figure 5 with the water uptake data in Table 1 for each of the three samples, one observes that nearly all of the water present in each of the samples was converted to hydrate. The discrepancies between the reconstructed pore volumes and that obtained from the nitrogen desorption studies are not the result of the

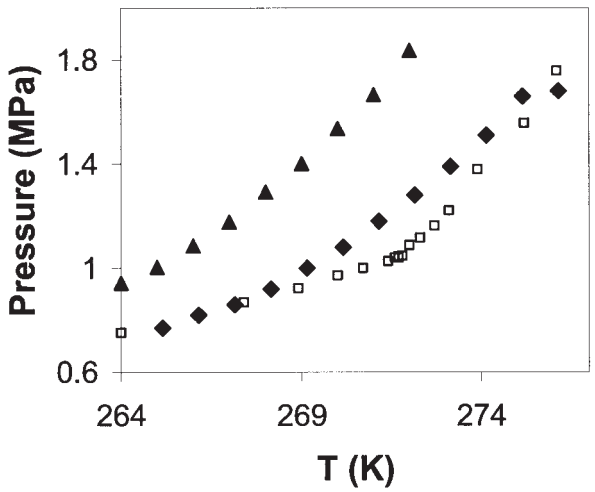

Figure 4. Measured equilibrium pressures (filled diamonds) for carbon dioxide hydrate in porous glass with a nominal pore radius of 15 nm, and for 7.5 nm silica gel (filled triangles) from the literature.

Also shown are data for bulk hydrate from Sloan (1997) (open squares).

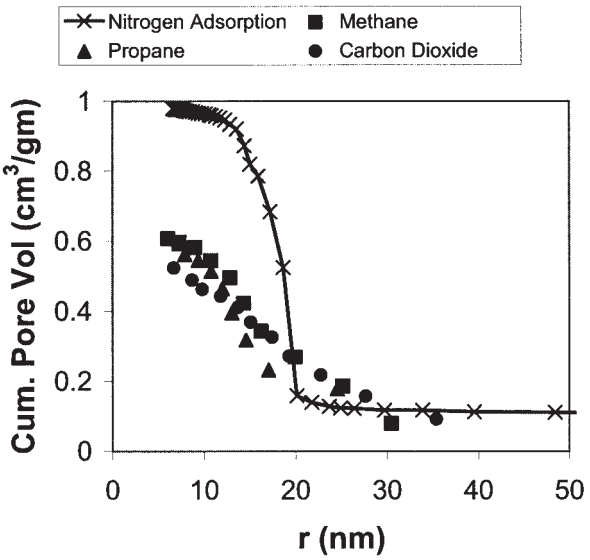

Figure 5. Comparison of cumulative pore-volume distributions based on nitrogen desorption studies and the hydrate equilibrium data from Figures 2–4.

failure to form hydrate in all water-containing pores, but result from not filling all of the pores in the glass with water before hydrate was formed. The cause for the discrepancy between the water uptake in this porous glass and the total pore volume as determined by nitrogen desorption is unknown. Similar differences have been reported between the amount of water adsorbed by natural porous media and the total pore volume of the media as predicted in nitrogen desorption studies, where the discrepancy was attributed to the presence of very narrow pores that resulted in the enhancement of nitrogen desorption, but had little influence on the water adsorption capacity (Gruszkiewicz, 1996). Our data suggest that only about 64.25% of the total pore volume was available for hydrate formation. Unfortunately, there are no experimental data available that would allow us to determine whether this observed difference in pore volume was attributed to the smallness of some of the pores, thereby retarding water adsorption in some localized areas of the medium but allowing nitrogen to pass freely, or to some other mechanism.

In the experiments reported in the current work, before hydrate formation the porous glass was allowed to equilibrate in a desiccator for the same amount of time as was previously used for silica gel (4–6 days). A longer equilibration time might give at least a somewhat larger fractional filling of the pores. The consistency of the water uptake data reported in Table 1, along with the agreement of the reconstructed pore volumes for the three different hydrates, suggests that the pore volume distributions represented in Figure 5 correspond to the distribution of water-filled pores before the formation of hydrate in the porous glass samples. We note that there is a slight discrepancy between the pore volumes at larger pore sizes (20–28 nm). It is unclear whether this difference is indicative of experimental differences between the two methods, or of the presence of transitory ice caps blocking off localized portions of the pore network until the temperature reaches a point above the melting point of water in the affected pores, thereby delaying the release of vapor from decomposing hydrate and causing an apparent shift of the pore volume distribution toward larger pore radii.

Figure 6 shows the pore volume distribution calculated from the methane hydrate equilibrium data of Figure 2. Because of the high percentage of water taken up by the porous glass that was converted to hydrate (about 97%), this can be taken as an indication of the distribution of all of the water in the porous glass. Also shown in Figure 6 are interpolated specific volumes obtained from the nitrogen desorption data. Both the hydrate data and the nitrogen desorption results indicate a specific volume of about 0.1 cm^3/g for radii above the ranges indicated in the figure. As is clear from Figure 6, most of the difference between the actual total pore volume (as determined from the nitrogen desorption study) and that obtained from the hydrate data is the result of a decrease in pore volume in the 15 to 20 nm range during the water-uptake portion of the experiments reported in this work. The specific cause for the failure of the larger pores to be completely filled with water is unknown, but may be a consequence of insufficient capillary forces to result in complete filling of all of the pore space, as discussed above. Because techniques such as nitrogen adsorption can indicate only the total pore-space, they are not useful in obtaining information about the distribution of water (and thereby hydrate) in the sample. Our method, on the other hand, allows for the determination of where hydrate was present, from which one can infer the presence (or absence) of water in a specific range of pore sizes; given that in many applications it is important to determine the distribution of water in the media (and not just the total pore volume), we believe this demonstrates a potential use for our method.

Comparison of sampled pore radii

Several groups of investigators (Clark et al. 1999; Henry et al., 1999; Klauda and Sandler, 2001) have attempted to model

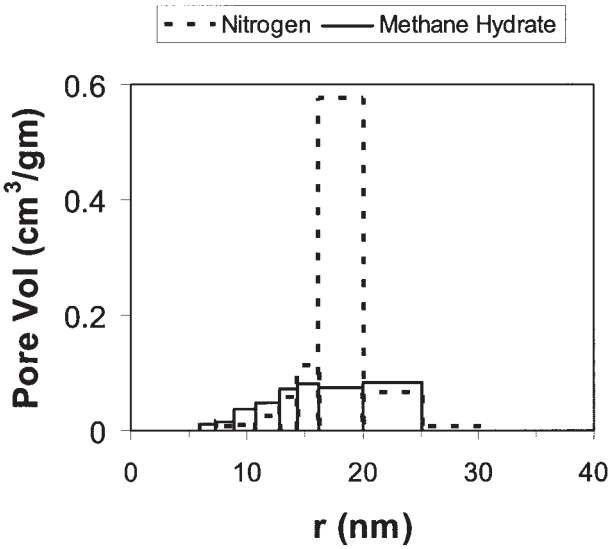

Figure 6. Comparison of the pore-volume distributions based on nitrogen desorption studies and the methane hydrate equilibrium data from Figure 2.

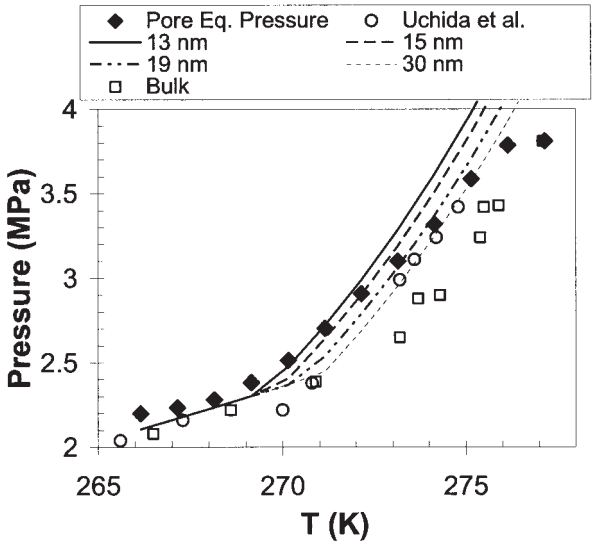

Figure 7. Experimental data from Figure 2 for methane hydrate in porous glass, with a nominal pore radius of 15 nm, along with calculations for various pore radii based on Eq. A4.

hydrate equilibrium pressures in porous media using a single pore size. Because of the presence of a distribution of pore sizes in the porous medium this is inherently unsatisfactory because each experimental pressure–temperature (P–T) point represents the equilibrium in a different size of pore. In most cases, the single-size treatment leads to unsatisfactory comparisons to experimental data. To circumvent this problem, Uchida et al. (1999) identified a unique experimental point, the point of maximum slope in the P–T diagram, with a unique pore radius, the mode of the distribution of pore radii.

Figure 7 shows the experimental data from Figure 2 for methane hydrate in porous glass. Also shown are predictions for several different (but constant) pore radii based on Eq. A4. Note that the experimental data reported in this work appear to have sampled a significant segment of the pore radii available in the porous glass. The last few data points before 276.15 K (where the hydrate was essentially exhausted) are relatively well fit by a single pore size of 19 nm, as one might expect based on the pore volume distribution in Figure 6, which shows a sharp cutoff of pore volume for radii above the 20–25 nm range. The relatively small amount of pore volume in pores larger than those in this range most likely accounts for the increase in equilibrium pressure, from 275.15 to 276.15 K, where the hydrate is completely exhausted.

If we examine the equilibrium pressures reported by Uchida et al. (1999) for methane hydrate in a similar porous glass (open circles in Figure 7), we see that they can be modeled by a single pore size over the whole range of the experimental temperatures reported in the literature. Although the exact reasons for the difference between the pore radii sampled during the hydrate decomposition experiments reported in the current work and those in the literature are unknown, possible contributing factors may be differences in the following: the nature or preparation of the hydrated porous glass samples; the nature of the decomposition experiments (continuous vs. discrete temperature rise); the sample to headspace ratios; and/or the equilibration times allowed for the water uptakes.

Further examination of the propane hydrate data

In hydrate decomposition experiments such as those described in this work, where a sequence of pressure measurements are made at ever increasing temperatures, one expects that at some temperature the equilibrium pressure will reach a plateau as a result of the complete dissociation of the hydrate in the sample. As the temperature is increased further, subsequent changes in the observed pressure will be attributable to the expansion of the gas already in the headspace of the cell. Figures 2 and 4 (which are for methane and carbon dioxide, respectively) show this expected behavior. Figure 3, however, shows a different behavior. At a temperature of 278.15 K, we note that the observed equilibrium pressure and that for the bulk hydrate seem to cross. Because capillary effects are known to increase equilibrium pressures (Henry et al., 1999), the crossing of the bulk and pore equilibrium pressure curves would normally be associated with the exhaustion of the pore hydrate (as can be seen in Figures 2 and 4 for the other guest species). If one exams the behavior above this temperature in Figure 3, it is clear, however, that as the temperature is increased the pressure rises more than can be ascribed to the expansion of the gas. The cause for this seemingly strange behavior becomes clear if one plots the vapor pressure of propane along with the observed experimental pressures, as has been done in Figure 8. In this figure, we plotted the bulk hydrate equilibrium pressure (Sloan, 1997) (small filled squares), the experimental pressures reported in this work (filled diamonds), and the bulk vapor pressure of propane (Yaws, 1977) (open squares). We note that the unusual behavior of the observed pressure begins roughly at the point of intersection of our hydrate pressure data with the propane

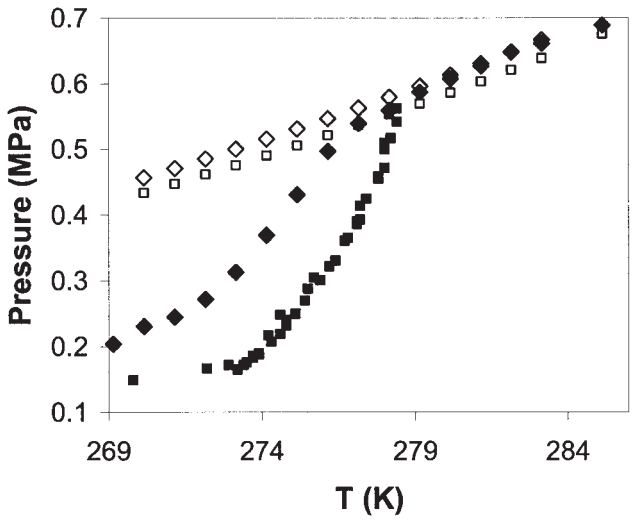

Figure 8. Experimental equilibrium data from Figure 3 for propane hydrate in porous glass (filled diamonds), bulk hydrate (filled squares), vapor–liquid equilibria for bulk propane (open squares), and vapor–liquid equilibria for propane in 16 nm pores (open diamonds).

vapor pressure curve. One possible explanation for the observed pressures beyond this point is that the pore hydrate was in fact exhausted at or before this pressure, and the experimental pressures beyond this point are actually the vapor pressure of the propane in the cell as a result of the cell pressure being above the dew point of propane. We note that there is a slight discrepancy between the observed pressures and the vapor pressure of propane reported in the literature (Yaws, 1977). We propose that this difference is the result of capillary effects on the vapor pressure of liquid propane in certain of the larger pores of the porous glass, as discussed below.

Note that the pore volume distribution for propane in Figure 5 (filled triangles) shows an appreciable amount of accessible pore volume in the 16 nm range that was not filled with water (and therefore not filled with hydrate at the start of the experiments). The presence of this unoccupied volume may help explain the difference between the experimental pressures in Figure 3 for temperatures above 278.15 K and the vapor pressure of propane. It is well known (Lupis, 1983) that the vapor pressure of a pure substance is affected by capillary effects. In fact, the vapor pressure (P^{vap}_{pore}) in a cylindrical pore of radius r is given in terms of the bulk vapor pressure (P^{vap}_{bulk}) by

$$\ln\left(\frac{P^{vap}_{pore}}{P^{vap}_{bulk}}\right) = \frac{V^{l}_{m}}{RT}\left(\frac{2\sigma}{r}\right) \tag{3}$$

where V^{l}_{m} is the molar volume of the liquid and σ is its surface tension. The pore vapor pressure of propane calculated from Eq. 3 using 16 nm for the pore radius has also been plotted in Figure 8. Values for the molar volume and surface tension at the necessary temperatures were taken from data available from the National Institute of Science and Technology. With the correction attributed to capillary effects, the curve representing the vapor pressure of propane in 16-nm pores shown in Figure 8 suggests that the pressures measured above 278.15 K may have resulted from the condensation of propane in pores having radii close to 16 nm. It seems plausible that the accessible pore volume near $r = 16$ nm in Figure 5 that was not filled with water initially (and which therefore did not contain hydrate during the propane hydrate decomposition experiment) may have acted as a reservoir for liquid propane once the pressure in the cell exceeded the vapor pressure in these pores, thus accounting for the observed pressure measurements between 278.15 and 285.15 K. This effect was not seen in the other experiments reported in this work because the vapor pressures of methane and carbon dioxide are greater than the respective hydrate equilibrium pressures for the temperatures reported in Tables 2 and 4.

Summary and Conclusions

Water uptake data reported in this work indicate that the volume of water taken up by porous glass pores of nominal 15 nm radii before the formation of hydrate was less than that expected from nitrogen desorption studies of this porous medium. Equilibrium pressures for the dissociation of methane, propane, or carbon dioxide hydrates confined in the porous glass pores were measured at various temperatures. Our data indicate that for each hydrate nearly all of the sorbed water was converted to hydrate. The measured equilibrium pressures were used to determine pore volume distributions based on a previously developed model. These reconstructed distributions were compared with those obtained from nitrogen desorption isotherms, and were used to indicate the distributions of water and hydrate among the various-sized pores of the glass. At higher temperatures, it was observed that in the case of propane hydrate, the pores not occupied by hydrate were involved in propane vapor–liquid equilibria.

Acknowledgments

This work was performed at the National Energy Technology Laboratory and was funded by the Office of Fossil Energy, U.S. Department of Energy.

Literature Cited

Barrett, E. P., L. G. Joyner, and P. P. Halenda, "The Determination of Pore Volume and Area Distribution in Porous Substances. 1. Computation from Nitrogen Isotherms," *J. Am. Chem. Soc.*, **73**, 373 (1951).

Clarke, M. A., M. Pooladi-Darvish, and P. R. Bishnoi, "A Method to Predict Equilibrium Conditions of Gas Hydrate Formation in Porous Media," *Ind. Eng. Chem. Res.*, **38**, 2485 (1999).

Clennell, M. B., M. Hovland, J. S. Booth, P. Henry, and W. J. Winters, "Formation of Natural Gas Hydrates in Marine Sediments 1. Conceptual Model of Gas Hydrate Growth Conditioned by Host Sediment Properties," *J. Geophys. Res.*, **104**, 22985 (1999).

Data were obtained from the National Institute of Science and Technology website using the applet located at gov.nist_chemdata.dv.DVApplet.

Elmer, T. H., "Porous and Reconstructed Glasses," Reprint from ASM International, Materials Park, OH (1992)

Gruszkiewicz, M. S., J. Horita, J. M. Simonson, and R. E. Mesmer, "Measurements of Water Vapor Adsorption on The Geysers Rocks," Proc. 21st Workshop on Geothermal Reservoir Engineering, Stanford University, Stanford, CA, January 22–24 (1996).

Handa, Y. P., and D. Stupin, "Thermodynamic Properties and Dissociation Characteristics of Methane and Propane Hydrates in 70-Å-Radius Silica Gel Pores," *J. Phys. Chem.*, **96**, 8599 (1992).

Henry, P., M. Thomas, and M. B. Clennell, "Formation of Natural Gas Hydrates in Marine Sediments 2. Thermodynamic Calculations of Stability Conditions in Porous Sediments," *J. Geophys. Res.* **104**, 23005 (1999).

Klauda, J., and S. I. Sandler, "Modeling Natural Gas Hydrate Phase Equilibria in Laboratory and Natural Porous Media," *Ind. Eng. Chem. Res.*, **40**, 4197 (2001).

Lowell, S., and J. E. Shields, *Powder Surface Area and Porosity*, Chapman & Hall, New York, Chapter 8 (1991).

Lupis, C. H. P., *Chemical Thermodynamics of Materials*, Elsevier, New York, Chapter 5 (1983).

Munck, J., S. Skjoid-Jorgensen, and P. Rasmussen, "Computations of the Formation of Gas Hydrates," *Chem. Eng. Sci.*, **43**, 2661 (1988).

Parrish, W. R., and J. M. Prausnitz, "Dissociation Pressures of Gas Hydrates Formed by Gas Mixtures," *Ind. Eng. Chem. Proc. Des. Dev.*, **11**, 26 (1972)

Seshadri, K., J. W. Wilder, and D. H. Smith, "Measurements of Equilibrium Pressures and Temperatures for Propane Hydrate in Silica Gels with Different Pore-Size Distributions," *J. Phys. Chem.*, **105**, 2627 (2001).

Sloan, E. D., *Clathrate Hydrates of Natural Gases*, 2nd edition, Marcel Dekker, New York (1997).

Smith, D. H., J. W. Wilder, and K. Seshadri, "Methane Hydrate Equilibria in Silica Gels with Broad Pore-Size Distributions," *AIChE J.*, **48**, 393 (2002a).

Smith, D. H., J. W. Wilder, and K. Seshadri, "Thermodynamics of Carbon Dioxide Hydrate Formation in Media with Broad Pore-Size Distributions," *Environ. Sci. Technol.*, **36**, 5192 (2002b).

Soave, G., "Equilibrium Constants from a Modified Redlich–Kwong Equation of State," *Chem. Eng. Sci.*, **27**, 1197 (1972).

Uchida, T., T. Ebinuma, and T. Ishizaki, "Dissociation Condition Measurements of Methane Hydrate in Confined Small Pores of Porous Glass," *J. Phys. Chem.*, **103**, 3659 (1999).

Uchida, T., T. Ebinuma, S. Takeya, J. Nagao, and H. Narita, "Effects of Pore Sizes on Dissociation Temperatures and Pressures of Methane, Carbon Dioxide, and Propane Hydrates in Porous Media," *J. Phys. Chem. B*, **106**, 820 (2002).

van der Waals, J. H., and J. C. Platteeuw, "Clathrate Solutions," *Adv. Chem. Phys.*, **2**, 1 (1959).
Wilder, J. W., K. Seshadri, and D. H. Smith, "Modeling Hydrate Formation in Media with Broad Pore-Size Distributions," *Langmuir*, **17**, 6729 (2001a).
Wilder, J. W., K. Seshadri, and D. H. Smith, "Resolving Apparent Contradictions in Equilibrium Measurements for Clathrate Hydrates in Porous Media," *J. Phys Chem.*, **105**, 9970 (2001b).
Wilder, J. W., and D. H. Smith, "Dependencies of Clathrate Hydrate Dissociation Fugacities on the Inverse Temperature and Inverse Pore Radius," *Ind. Eng. Chem. Res.*, **41**, 2819 (2002).
Yaws, C. L., "Physical Properties," *Chemical Engineering*, McGraw-Hill, New York, 99214 (1977).
Zhang, W., J. W. Wilder, and D. H. Smith, "Interpretation of Ethane Hydrate Equilibrium Data for Porous Media Involving Hydrate-Ice Equilibria," *AIChE. J.*, **48**, 2324 (2002a).
Zhang, W., J. W. Wilder, and D. H. Smith, "Equilibrium Pressures and Temperatures for Equilibria Involving Hydrate, Ice, and Free Gas in Porous Media," *Proc. 4th International Conf. Gas Hydrates*, Yokohama, Japan (May 19–23, 2002b).

Appendix

Modeling hydrate equilibria in porous media

Numerous authors have presented statistical thermodynamic models based on variations of the van der Waals–Platteau equation. Munck et al. (1988) used a previously developed model (Parrish and Prausnitz, 1972) to obtain a single equation involving T_f and P_f (the temperature and pressure under which the hydrate forms) that can be used to predict hydrate formation conditions. In the case of hydrates formed from mixtures this equation takes the form

$$\frac{\Delta\mu_{W_0}}{RT_0}-\int_{T_0}^{T_f}\frac{\Delta H_w}{RT^2}\,dT+\int_0^{P_f}\frac{\Delta V_w}{R\bar{T}}\,dP-\ln(\gamma_w X_w)+\sum_i \eta_i\ln\left(1-\sum_k Y_{ki}\right)=0 \quad \text{(A1)}$$

In Eq. 3, $\bar{T} = (T_0 + T_f)/2$, T_0 is the temperature of the standard reference state ($T = 273.15$ K, $P = 0$), $\Delta\mu_W^0$ is the chemical potential difference between the empty hydrate lattice and pure water in the reference state, η_i is the ratio of the number of cavities of type i to the number of water molecules in the hydrate lattice, and Y_{ki} denotes the probability of a cavity of type i being occupied by the guest molecule type k. The probability Y_{ki} is given in terms of the fugacity of the hydrate guest (f_k) in the gaseous state (calculated using the Soave–Redlich–Kwong equation of state) and the Langmuir adsorption constant (C_{ki}) by

$$Y_{ki} = \frac{C_{ki}f_k}{1 + \sum_j C_{ji}f_j} \quad \text{(A2)}$$

Additionally, $\Delta H_W = \Delta H_W^0 + \int_{T_0}^{T}\Delta C_p(T')dT'$, where ΔH_W^0 is a reference enthalpy difference between the empty hydrate lattice and the pure water phase at the reference temperature, $\Delta C_p(T')$ is assumed constant (van der Waals and Platteeuw, 1959) and equal to ΔC_p^0 (the reference heat capacity difference), and ΔV_W is the volume difference between the empty hydrate and pure water (at T_0), and is assumed constant. Also note that the values used for ΔC_p^0, ΔH_W^0, and ΔV_W depend on whether the equilibrium involves liquid or solid water. Munck et al. (1988) and Parrish and Prausnitz (1972) accounted for the temperature dependency of the Langmuir constants by using the functional form

$$C_{ki} = \frac{A_{ki}}{T\exp(B_{ki}/T)} \quad \text{(A3)}$$

where A_{ki} and B_{ki} are experimentally fit parameters, and are dependent on which guest molecule is present, as well as which of the three hydrate structures is formed.

To describe hydrate formation in porous media, Eq. A1 must be modified to include the effect of the relevant interface on the activity of the water. After making the necessary modifications in the region where the equilibria involve liquid water, Eq. A1 becomes (Henry et al., 1999)

$$\frac{\Delta\mu_W^0}{RT_0}-\int_{T_0}^{T_f}\frac{\Delta H_w}{RT^2}\,dT+\int_0^{P_f}\frac{\Delta V_w}{R\bar{T}}\,dP-\ln(\gamma_w X_w)+\sum_i \eta_i\ln\left(1-\sum_k Y_{ki}\right)+V_L\frac{2\cos(\theta)\sigma}{RT_f r}=0 \quad \text{(A4)}$$

We note that Clarke et al. (1999) presented a similar equation based on the assumption of a different interface, whereas Klauda and Sandler (2001) used a slightly different model formulation. In Eq. A4, V_L is the molar volume of water in the aqueous phase, θ is the contact angle between the aqueous phase and the hydrate, σ is the surface tension of the relevant interface involving the hydrate phase (that is, that between the hydrate and the relevant aqueous phase), and r is the radius of a pore in the porous medium. Because the solubility of most guests in water is small, these parameters are approximated by their values for pure water. Equation A4 can be used for all temperatures, although some of the parameters will have different values, depending on whether the temperature is above or below the quadruple point in the corresponding pore of radius r. Below this temperature one recovers the same equation as that given above for the bulk, given that the current model assumes there are no surface affects between ice and hydrate (Wilder and Smith, 2002), as was recently verified experimentally (Zhang et al., 2002a).

Most attempts by other groups to use this type of model to interpret hydrate data involving porous media have been less than satisfactory because of their use of a single pore size to characterize the porous media. In a series of articles our group has applied a conceptual model in which it is recognized that each P–T data point corresponds to an equilibrium involving a unique (but changing) pore size as one increases the cell temperature and allows equilibrium to be reestablished in the cell by the decomposition of hydrate from the sample. In applying this model, one can use the experimental temperature and pressure in Eq. A4 for P_f and T_f, respectively, along with standard values of the other parameters, leaving the only unknown quantity to be $\cos(\theta)\sigma/r$. Solving for this quantity from Eq. A4 in the case where the equilibrium involves liquid water yields

$$\frac{\cos(\theta)\sigma}{r} = \frac{RT_f}{2V_L}\left[\frac{\Delta\mu_W^0}{RT_0} - \int_{T_0}^{T_f}\frac{\Delta H_w}{RT^2}\,dT + \int_0^{P_f}\frac{\Delta V_w}{R\bar{T}}\,dP - \ln(\gamma_w X_w) + \sum_i \eta_i \ln\left(1 - \sum_k Y_{ki}\right)\right] \quad \text{(A5)}$$

To use Eq. A5 to determine the pore size in equilibrium at a specific temperature, one must first pick a value for the surface tension, σ, as well as for the cosine of the contact angle. In this work we assume that for equilibria involving liquid water $\cos(\theta)$ is unity. Although various authors (Henry et al., 1999; Klauda and Sandler, 2001; Uchida et al., 1999, 2002) have proposed several different values for the surface tension, our work suggests that the value of the surface tension between liquid water and hydrate may not be significantly different from that between water and ice. As a result, similar to Henry et al. (1999), we shall use a value of 0.0267 N/m^2. Because the only unknown left in Eq. A5 is the pore radius, one can rearrange Eq. A5 to give

$$r = -\frac{2V_L\cos(\theta)\sigma}{RT_f\left[\frac{\Delta\mu_W^0}{RT_0} - \int_{T_0}^{T_f}\frac{\Delta H_w}{RT^2}\,dT + \int_0^{P_f}\frac{\Delta V_w}{R\bar{T}}\,dP - \ln(\gamma_w X_w) + \sum_i \eta_i \ln\left(1 - \sum_k Y_{ki}\right)\right]} \quad \text{(A6)}$$

which can be used to determine the radius (r) of the pores involved in the equilibrium, leading to the observed equilibrium pressure (P_f) at the specified experimental temperature (T_f). The values for the parameters in Eq. A6 were previously reported in the literature (see Table 2 in Smith et al., 2002a and Table 3 in Smith et al., 2002b). Note that Eq. A6 is valid only for equilibria involving liquid water.

Manuscript received Mar. 20, 2003, and revision received Sep. 28, 2003.